Displacement field normalization in MR-elastography: phantom validation and *in vivo* application

Marion Tardieu[1], Marie Poirier-Quinot[1], Ralph Sinkus[2], Luc Darrasse[1], and Xavier Maître[1]
[1]*IR4M (UMR8081), CNRS, Univ Paris-Sud, Orsay, France,* [2]*Imaging Sciences & Biomedical Engineering Division, King's College, London, United Kingdom*

Purpose

MR-elastography aims at characterizing the mechanical properties of living tissues by probing wave propagation therein. Displacement fields are recorded over a mechanical cycle by encoding the inferred motion along the three spatial directions. Thus the complex shear viscoelastic moduli can be computed after inversion of the wave equation[1]. Patients' motion during the MR-acquisition usually results in unrestrained spatial transformations of the targeted organ. It may also yield unwanted mismatch of the components of the acquired displacement fields. Spatial normalization of the phase image along the magnitude image tackles the correcting linear or non-linear transformations but, as numerically showed recently[2], displacement field normalization is required to fully recover the phase information in MR-elastography and improve the parametric reconstruction. Here, we experimentally validate the approach by applying these corrections on a breast phantom after MR-elastography exams for arbitrary three-dimensional rotations. This double normalization scheme was advantageously applied on a brain MR-elastography data set where the subject had involuntary moved during the acquisition.

Materials and methods

Breast phantom MR-elastography acquisitions: Acquisitions were performed in a 1.5 T scanner (Achieva, Philips, The Netherlands). Pressure waves were remotely generated by a loudspeaker at 120 Hz and transmitted to the surface of a breast phantom (Model 051, CIRS, USA) along a waveguide[3]. A set of three spin-echo sequences with motion encoding gradients of 21 $mT.m^{-1}$ along the three spatial directions was implemented with FOV = 140×80×93 mm^3, matrix = 80×52×40, TE/TR = 37/2333 ms, and four dynamics to sample the displacement fields along the oscillatory period. As spatial translations do not affect the displacement fields, only three-dimensional rotations were applied to the phantom by simply rotating the field of view along the three anatomical axes concurrently by 5, 10, 13, and 15°. The full protocol was performed three times to evaluate the reproducibility of the methodology. Default phase corrections were removed.

Brain MR-elastography acquisitions: Acquisitions were performed along the same lines as for the breast phantom but with FOV = 264×154×118 mm^3, matrix = 96×96×43, TE/TR = 48/3803 ms, and pressure waves guided to the subject's buccal cavity at 113 Hz.

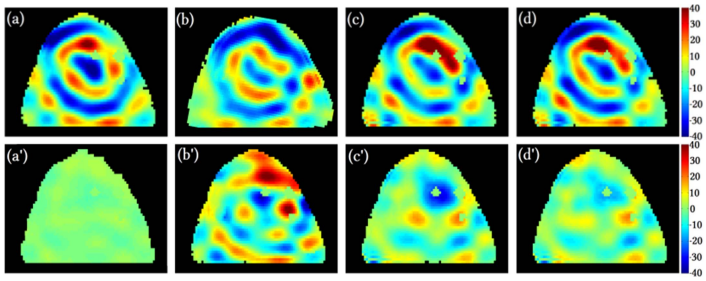

Figure 1: Top row: Displacement maps (µm) of the reference acquisition (a), 10° rotated acquisition (b), after spatial normalization (c), and after displacement field normalization (d). Bottom row: Difference displacement maps (b',c',d') between the reference acquisition map (a) and the corresponding maps from the top row (b,c,d). Difference displacement map (a') between (a) and a repeated acquisition. Central slice of the breast phantom.

Spatial and displacement corrections: Spatial normalization was performed on the rotated acquired data set using SPM8 (UCL, London, UK), with the 0°-rotated data set as a template. The transformation matrix was constructed from the inferred angles and was applied to the spatially normalized components of the displacement fields.

Data processing: For each acquisition, phase was unwrapped before computing the displacement field maps. SNR maps were calculated to produce corresponding phase-error maps ($\Delta\Phi = \operatorname{atan} \mathrm{SNR}^{-1}$) and field displacement-error maps ($\propto \Delta\Phi$)[4]. The reproducibility was estimated by the averaged standard deviation over the difference between the displacement maps of every three acquisitions that were repeated. Rotated data sets were simulated from the reference displacement maps for comparison. The processing efficiency was measured along the mean standard deviation over the difference between reference and rotated field displacement maps.

Results

For breast phantom images, the displacement field total magnitude reached 68.2 µm. The SNR was 82.6±16.6 such that phase errors were expected between 0.6° and 0.9° and displacement fields were measured within 0.25 µm and 0.38 µm. Two repeated MR-elastography measurements presented field displacement maps within ±2 µm. Field displacement maps and corresponding difference maps are presented in Figure 1 for a 10° rotated FOV. Figure 2 shows the evolution of the processing efficiency. For brain images, the recorded subject's motion introduced rotations with angles up to 2°. The complex viscoelastic parametric maps (G=G'±iG") as well as the difference maps with and without normalizations are shown on Figure 3. Discrepancies close to ±0.23 kPa and ±0.20 kPa are revealed in G' and G" maps, respectively.

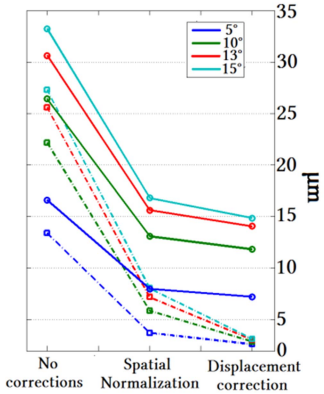

Figure 2: Evolution of the mean standard deviation of the difference between the static and the rotated data sets after spatial and field displacement normalization for 5°, 10°, 13°, and 15°, at 120 Hz, for experimental (solid lines)and simulated (dotted lines) data sets.

Discussion

The error induced on the displacement fields obviously increases with the rotation angle as does the processing efficiency. For simulated noise-free rotated datasets, double normalization processing is virtually fully efficient. It remains efficient for experimental datasets by reducing the remaining displacement field deviation down by more than a factor 2. Most of the work is carried by the spatial normalization but the displacement field normalization still brings more than 10% improvement. When dealing with surface deformation, a 10° rotation angle for the breast phantom corresponds to a 4° head rotation, which motion is commonly encountered in clinical practice. As shown earlier[2], the viscoelastic maps obtained here in the brain require spatial and displacement field normalizations, even for small-rotation-induced translation. Such normalizations may be highly beneficial for some inherently-moving organs like liver.

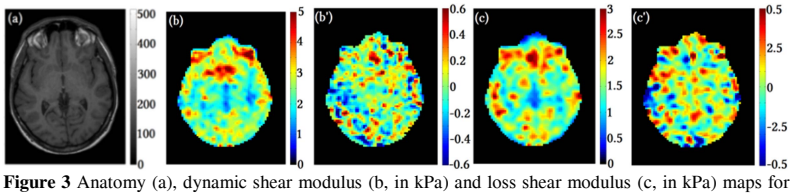

Figure 3 Anatomy (a), dynamic shear modulus (b, in kPa) and loss shear modulus (c, in kPa) maps for one of the 43 slices of motion-fully-corrected brain elastography data of a healthy subject. Difference maps with and without spatial and field displacement normalizations for G' (b', kPa) and G" (c', in kPa).

References

1. Sinkus *et al.* Magn Reson Imaging **23**:159-165 (2005) 2. Tardieu *et al*. in *ISMRM* 2013:3099 Salt Lake City, USA 3. Maître *et al.* in *ISMRM* 2011 Montréal, Canada 4. Muthupillai *et al.* Science **269**:1854-1857 (1995)